Desalination and Water Treatment 318 (2024) 100405

Contents lists available at ScienceDirect

Desalination and Water Treatment

journal homepage: www.sciencedirect.com/journal/desalination-and-water-treatment/

Date palm fiber agro-waste biomass for efficient removal of 2,4,6-Trichlorophenol from aqueous solution: Characterization, Kinetics, Isotherms studies and Cost-effective analysis

Nadavala Siva Kumar[a,*], Mohammad Asif[a], Anesh Manjaly Poulose[b], Ebrahim H. Al-Ghurabi[a], Shaddad S. Alhamedi[a], Janardhan Reddy Koduru[c]

[a] Department of Chemical Engineering, College of Engineering, King Saud University, P.O. Box 800, Riyadh 11421, Saudi Arabia
[b] Department of Chemical Engineering, SABIC Polymer Research Centre, King Saud University, P.O. Box 800, Riyadh 11421, Saudi Arabia
[c] Department of Environmental Engineering, Kwangwoon University, Seoul 01897, Republic of Korea

ARTICLE INFO

Keywords:
Date palm Fiber
2,4,6-trichlorophenol
Adsorption
Chemical modification
Kinetics and isotherms modeling

ABSTRACT

This study proposes using date palm biomass to remove emerging industrial contaminants, such as 2,4,6-Trichlorophenol (2,4,6-TCP) from water, promoting sustainable waste utilization and a more cost-effective technology. To investigate the potential of using raw date palm fiber and Triethylamine-modified date palm fibers (RDPF and TEA–MDPF) for 2,4,6-TCP removal in batch adsorption experiments. The residual concentration of 2,4,6-TCP in the effluents was examined using UV–visible spectroscopy. The structural and chemical composition of the raw and modified biomass materials was determined using various techniques, including BET, FTIR, Elemental analyzer (CHN), Particle size analysis, FESEM-EDX, and TGA analysis. The optimal pH for the highest 2,4,6-TCP uptake capacity in batch equilibrium adsorption studies was found to be 2.0 for RDPF and 6.0 for TEA-MDPF biomass. The sorption kinetics of 2,4,6-TCP onto both adsorbents was excellent, designated by the pseudo-second-order (R^2 = 0.93–0.99) and Elovich models (R^2 = 0.86–0.97). This indicates that adsorption was regulated by chemisorption. The results of the experiment exhibited a good correlation (R^2) between the PSO and the maximum (q_m) uptake capacities of the Langmuir isotherm model for the remediation of 2,4,6-TCP from aqueous media, which was 115.50 mg/g and 191.75 mg/g for RDPF and TEA-MDPF, respectively. TEA-MDPF biomass exhibits superior adsorption capacity compared to RDPF, making it a promising candidate for the remediation of 2,4,6-TCP from aqueous contaminated wastewater.

1. Introduction

Water safety is of utmost importance nowadays for both humans and the ecosystem. Chlorophenol compounds (CPs) are often found in water due to the discharge of polluted wastewater from various industrial, domestic, and agricultural sources [1]. Among these CPs, 2,4,6-Trichlorophenol (2,4,6-TCP) is mostly used in agriculture, wood preservation, and organic compound synthesis as pesticides, fungicides, herbicides, and more. 2,4,6-TCP pollution can degrade the quality of water, posing risks to human health and aquatic life, including cancer, deformity, and mutation. Chemical structure of 2,4,6-TCP makes it difficult to degrade, foremost to high toxicity, bioaccumulation, carcinogenicity, long-distance migration, and dangerous secondary pollution during treatment [2–4]. Therefore, it is essential to treat 2,4,6-TCP strictly before discharging it into the water circulatory system to prevent its harmful effects on the environment and human health, even at low concentration levels.

Over the past decade, various successful wastewater analytical treatment techniques have been used to remediate CPs, such as solvent extraction, biodegradation, catalytic ozonation, ion exchange, and photochemical degradation [5–11]. Among all these methods, certain disadvantages include costliness and ineffectiveness; thus, these techniques are not appropriate for operating at small industries' scale level. Adsorption is a highly recommended method for remediating phenolic derivatives from wastewater due to its simplicity, eco-friendliness, affordability, efficacy, and reusability when compared to other methods, and it is frequently used at an industrial scale [12,13]. Although commercially existing activated carbon has a high surface area and sorption capacity, it is a costly system with high operational expenses, which needs regeneration after every cycle. To tackle the issue of phenol and

* Corresponding author.
E-mail address: snadavala@ksu.edu.sa (N.S. Kumar).

https://doi.org/10.1016/j.dwt.2024.100405
Received 12 March 2024; Received in revised form 13 May 2024; Accepted 19 May 2024

chlorophenol remediation, researchers aim to develop unconventional, cheap, effective, and locally available sorbents. So far, various studies have examined the adsorption of phenol and chlorophenols on agricultural and natural resource materials [2,12,14–17]. Lignocellulosic biomass is a readily available and inexpensive bio-adsorbent with the potential for effective remediation of heavy metals and organic pollutants [18–20]. Recent studies have shown that agricultural waste and lignocellulosic residues possess high sorption capacities and do not require frequent regeneration, making them a cost-effective solution for wastewater treatment [21,22]. Nevertheless, there is still a lack of investigation on the use of agro-waste lignocellulose biomass materials for the remediation of phenol and its derivatives from aqueous wastewater.

Utilizing lignocellulose biomass from the date palm plant is an exceptional solution for removing organic pollutants. The date palm fiber waste biomass is easily available locally and highly abundant in Saudi Arabia [23]. Date palm fiber lignocellulose biomass contains lignin (15–35 %), cellulose (40–50 %), and hemicellulose (20–35 %) components [24]. Moreover, it is a cost-effective substitute for other adsorbents utilized in treating aqueous wastewater. Date palm fibers have been successfully employed for the eradication of heavy metals [25–28], dyes [29–31], phenol, and nitrate pollutants [21,32–34]. However, to our knowledge, no reports exist on the use of raw or chemically modified date palm fiber biomass for 2,4,6-TCP pollutant remediation in wastewater.

Here this present study evaluates the demonstration of raw and TEA-chemically modified date palm fibers (RDPF and TEA-MDPF) as an adsorbent for remediating 2,4,6-trichlorophenol. To investigate the impact of different operational conditions, such as solution pH, agitation time duration, adsorbent quantity, and adsorbate concentration, by conducting equilibrium batch studies. Throughout the study, we meticulously analyzed the samples using various techniques such as elemental analyzer (CHN), BET surface area, SEM, particle-size analyzer, TGA, and FTIR analysis. We aimed to instigate a correlation between the properties of the adsorbent and its effectiveness in removing pollutants.

2. Materials and methods

2.1. Chemicals

The 99 % pure 2,4,6-trichlorophenol was obtained from Sigma-Aldrich (St. Louis, Missouri, United States) and used. The molecular formula of 2,4,6-TCP is C6H2Cl3OH, and its molecular weight is 197.45 g/mol. To make stock solutions, 1.68 g of chlorophenol was dissolved in 1000 mL of distilled water. This stock solution was then used to obtain the required working concentration in the range of 50–200 mg/L for experiments. To adjust the pH of this solution, 0.1 M HCl and 0.1 M NaOH were used.

2.2. Collection and preparation of date-palm fiber biomass

The agro-waste date palm fiber (DPF) biomass material was collected from the region of Riyadh, Saudi Arabia. The DPF was cleaned with normal tap water to eliminate the impurities and then dried for 2 days in daylight. After cleaning the DPF, it was cut into 2–4 cm pieces, crushed with a milling device, and allowed through a 0.4 mm sieve. Next, the RDPF was ground using a grinder (DLC multifunctional) and sieved to obtain a fine powder. After that, sieved powder was collected and ground using a Fritsch ball-milling device (Premium line, Pulverisette 7, Germany). The grinding process involved using steel balls (zirconia ceramic) at 400 rpm for 24 h. Additionally, the micro ball-milling device was utilized at 1500 rpm for 30 min (POWTEQ Laboratory, GT300, Beijing, China). The label RDPF has been assigned to the sample of date palm fiber that has undergone micro ball-milling.

2.3. Chemical modification of RDPF

The RDPF powder was subjected to chemical modification with triethylamine. This procedure was adapted from Song et al., 2015 and slightly altered [35]. Specifically, the Song et al. described method was modified to some extent to achieve the desired results. 10 g of raw date palm fiber powder were mixed with 100 mL of triethylamine and methanol. The obtained blend was stirred for an hour at room temperature while maintaining an agitation speed of 200 rpm. Afterward, the modified mixture was washed with distilled water and dried up for 24 h at 110 ˚C. The chemically modified palm fiber sample was then labeled as TEA-MDPF and kept in a desiccator for future experimental adsorption studies.

2.4. Batch studies

The concentration of 2,4,6-TCP was varied from 50–200 mg/L in a series of batch experiments. A 100 mL solution containing 0.1 g RDPF and TEA-MDPF biomass was placed in a 125 mL (amber glass) reagent bottle. We agitated the samples at 30 ± 1 ˚C in a shaker (Grant, OLS Aqua Pro, water bath) at 175 rpm until a steady state was achieved. The solution pH was altered from 2–10. To obtain the supernatant solution for filtration, Whatman No-41 filter paper was used. TCP concentration was determined at 296 nm through a UV-1900 (Shimadzu, Tokyo, Japan) UV–VIS Spectrophotometer.

To optimize the sorption (q_e, mg/g) capacity and remediation efficiency, the subsequent equations were employed,

$$q_e = \frac{(C_0 - C_e)V}{W} \tag{1}$$

$$Removal(\%) = \frac{(C_0 - C_e) \times 100}{C_0} \tag{2}$$

where, C_0 = concentration of TCP (mg/L) at time = 0, q_e = sorption capacity at equilibrium, C_e = TCP equilibrium concentration (mg/L) at V = solution volume (L), W = RDPF and TEA-MDPF mass (g).

In the batch kinetic experiments analysis, we calculated the TCP sorption, qt (mg/g), at various time intervals.

$$q_t = \frac{V(C_0 - C_t)}{W} \tag{3}$$

where C_t is the solute concentration (mg/L) at time, t (min). The evaluation of equilibrium kinetic and isotherm models, using chi-square analysis and normalized standard deviation, is defined in detail in Supplementary Materials Section 2.4.

2.5. Biomass characterization techniques

Various techniques were employed to analyze the properties of the biomass-based adsorbent. A detailed description of these techniques is provided in sections 2.5.1 to 2.5.7 of the Supplementary Materials. The Point of zero charge (pHpzc), particle size, C, H, N analysis. BET analysis were used to study the particle size, average pore size, pore volume, and surface area. The surface functional groups of the RDPF and TEA-MDPF adsorbents were identified using the FTIR method. The stability of the raw and modified adsorbent was assessed using thermogravimetric analysis (TGA). The FESEM-EDX was utilized to analyze the morphology of the biomass.

3. Results and discussion

3.1. Characterization of RDPF and TEA-MDPF

3.1.1. Particle size data analysis

To increase a better understanding of the process of reducing size, we measured the particle size of RDPF biomass samples. We analyzed

Table 1
Composition data (C, H, N, O) on RDPF and TEA–MDPF adsorbent.

S. No	Biomass	C (%)	H (%)	N (%)	O (%)
1	RDPF	46.13	5.98	0.05	47.84
2	TEA–MDPF	44.58	3.64	0.80	50.98

the distribution size of two reduction size procedures, namely 24-hour (ball-milling) and 30-minute (micro-ball-milling), using cumulative and differential volume percentages. Our previously published work contains these results, which are also available in the supplementary section Figs. S1-S2 [21].

3.1.2. Composition analysis

Table 1 displays the confirmed elemental composition (C, H, N, O (carbon, hydrogen, nitrogen, and oxygen)) in biomass obtained from RDPF and TEA-MDPF. Additionally, there was a slight decrease in the carbon and hydrogen (%) contents of the TEA-MDPF samples. Several other researchers have obtained similar results in their investigations [21,36].

3.1.3. FTIR data analysis

Fig. 1 displays the FTIR spectrum peaks of RDPF and TEA-MDPF biomass structure, identifying bands in the 4000–400 cm^{-1} range. Fig. 1(a-d) exhibits the broadband peaks at around 3424–3447 cm^{-1}, and it indicates the band is associated with the existence of O-H (hydroxyl group) stretching vibrations due to hydrogen bonding, such as lignin and cellulose. The RDPF biomass peaks at 2931 cm^{-1} might be assigned to C–H stretching vibrations of $–CH_2$ and $–CH_3$ groups [37]. After the modification of TEA biomass, the vibration frequency of $–CH_2$ groups shifted to 2906 cm^{-1} [38]. The bands at 1374–1377 cm^{-1} correspond to the stretching of C-H bonds of acetyl groups found in hemicellulose esters. The chemically modified FB-TEA sample exhibits a peak around 1735 cm^{-1} (C═O). The stretching frequencies of C═C (1608–1641 cm^{-1}), CO-O-CO (1033–1058 cm^{-1}), C–Cl (600–850 cm^{-1}), and bending frequencies C═C (889–895 cm^{-1}) designate the presence of conjugated alkene, anhydride, functional groups, respectively. After the adsorption of 2,4,6-TCP onto the RDPF and TEA-MDPF biomass, no considerable changes in the peak positions were detected.

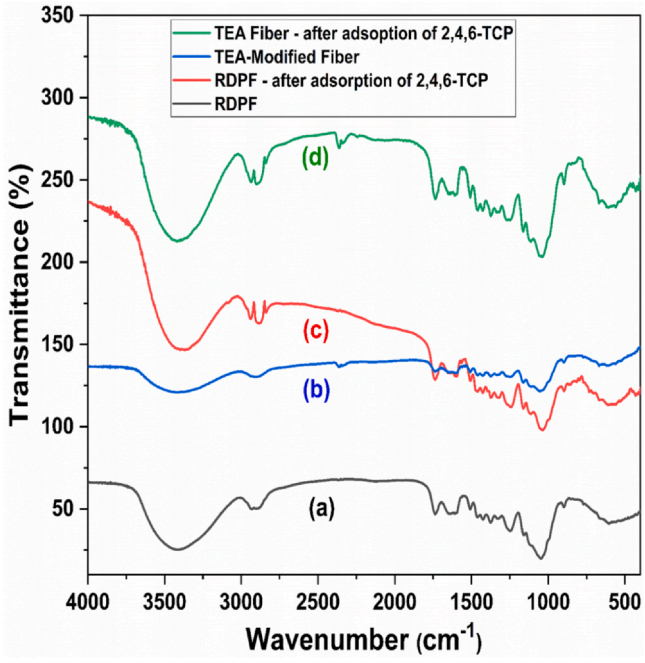

Fig. 1. FTIR spectra analysis of (a) RDPF, (b) TEA–MDPF, (c) after adsorption of 2,4,6-TCP, (d) TEA–MDPF after adsorption of 2,4,6-TCP.

3.1.4. BET Analysis

Figures (S3-S6) display the N_2 adsorption/desorption isotherm curves for ground DPF, 24-hr, micro ball-milled (RDPF), and TEA-MDPF powder samples. Table 2 presents the BET pore size, pore volume, and surface area of biomass samples. Before chemical modification, the micro ball-milled (RDPF) sample had an initial surface area of 3.555 m^2/g. However, after the triethylamine (TEA) chemical modification, the properties and characteristics of the sample were significantly reduced. The surface area decreased several-fold to 0.1482 m^2/g, and the pore volume decreased to 0.0023 cm^3/g. At the same time, the pore size reduced to 186 Å from 1197 Å, indicating the development of small pores due to the chemical modification. Similar behavior was observed in surface-modified lignocellulosic material and surfactant-modified montmorillonite, which also showed a decrease in BET surface area [39,40].

3.1.5. FESEM–EDX analysis

The FE-SEM images evaluated the surface morphology of RDPF and TEA-MDPF biomass. Figs. 2(a) and 3(a) depict the appearance of the biomass surface. The micrographs demonstrated that the surface of RDPF is more homogeneous than the rough surface of TEA-MDPF, which contains irregularly shaped particles with a porous surface area and many micropores and cavities. The rough surface of the chemically treated biomass may boost the adsorption capability of phenolic compounds. The EDX elemental composition (C, O) analysis validated the final composition (C, H, N) of RDPF and TEA-MDPF, as illustrated in Figs. 2(b-c) and 3(b-c).

3.1.6. TGA analysis

Fig. 4 shows the thermal analysis (TGA) of the raw and modified date palm fiber (RDPF and TEA-RDPF) biomass. Both TGA curves display three distinct weight loss regions. At around 100 °C, the weight loss is caused by the dehydration of moisture contained by the adsorbent itself. It is worth noting that both date palm fibers experience a 5–7 % loss in mass due to their hygroscopic nature and moisture [41]. During the weight loss of the second stage process in RDPF and TEA-MDPF, a significant portion was observed due to the decomposition of main components such as lignin, cellulosic, and hemicelluloses [42]. This weight loss occurred in the temperature range of 330–350 °C for both samples. The 50 % weight loss was observed at 330 °C for RDPF, while the TEA-MDPE exhibits around 350 °C. This is due to the effect of chemical modifications of the adsorbent [43,44]. At the final stage, it was observed that the residual biomass for the sample RDPF at 1000 °C remained at approximately 5 %, while modified samples showed almost double the amounts at similar temperatures.

3.2. Influence of adsorption parameters

3.2.1. Effect of pH

The adsorption capacity of RDPF and TEA-MDPF is important and pretentious based on the solution pH. To study its effect, the pH of the solution range was altered from 2–10, and the uptake capacity of 2,4,6-TCP was evaluated. Fig. 5a-b displays the results that the uptake capacity of RDPF decreased from 40.82–36.42 mg/g, and that of TEA-MDPF increased from 38.69–44.78 mg/g as the pH solution increased from 2–6. Further, a rise in the pH solution resulted in a reduction in the uptake efficiency of 2,4,6-TCP. The point of zero charge (pHpzc) analysis was used to determine the surface charge of the adsorbent. This is important because the pHpzc highly affects the adsorption of adsorbate onto the adsorbent. Any change in the surface charges of the adsorbent can significantly impact the adsorption process. In the case of RDPF and TEA-MDPF, the value of pHpzc was found to be in an acidic medium at 6.4 and 6.9, respectively. Below this pH, the surface of the adsorbents becomes positively charged, resulting in electrostatic attractions between the positively charged adsorbents and 2,4,6-TCP molecules. This means that the adsorption of 2,4,6-TCP occurs more

Table 2
BET analysis data of date palm fiber biomass material.

S. No	Adsorbent	Surface Area (m^2/g)	Pore Volume (cm^3/g)	Pore Size (Å)
1	Ground raw date-palm fiber	0.889	0.006	559.9
2	24 hrs ball-milled	2.016	0.009	238.2
3	RDPF	3.554	0.017	186.0
4	TEA–MDPF	0.148	0.002	1197

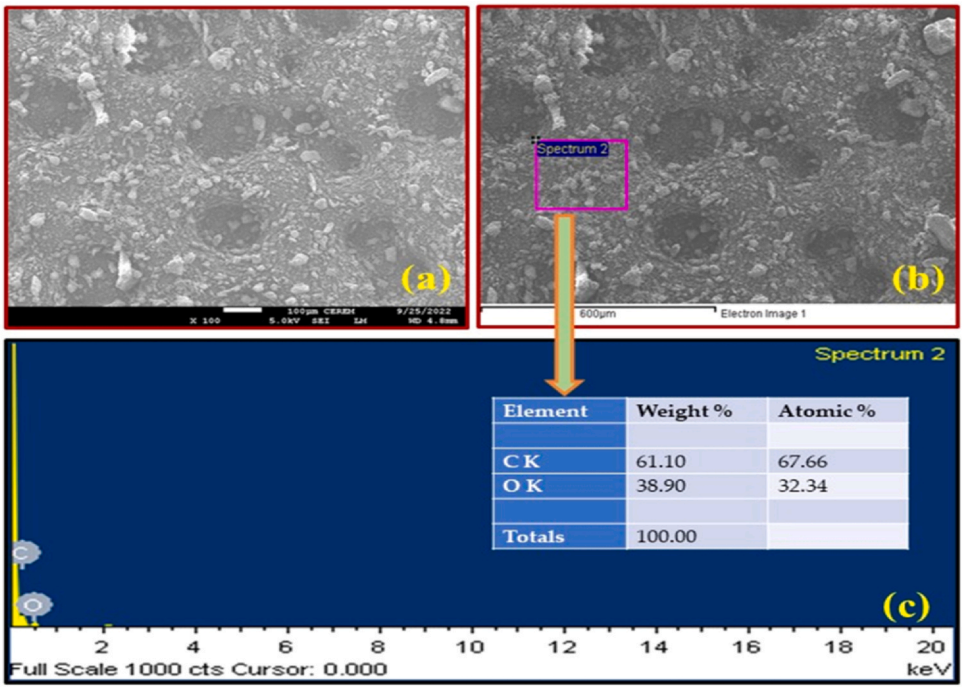

Fig. 2. FESEM-EDX images of raw date palm fiber (RDPF) biomass.

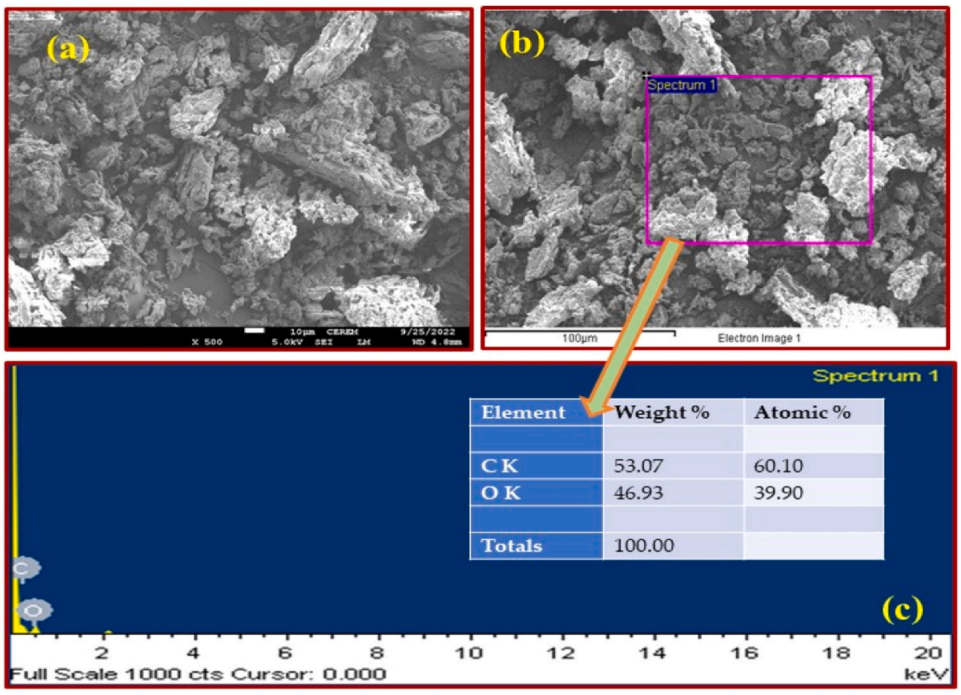

Fig. 3. FESEM-EDX images of TEA-chemical modified date palm fiber biomass (TEA–MDPF).

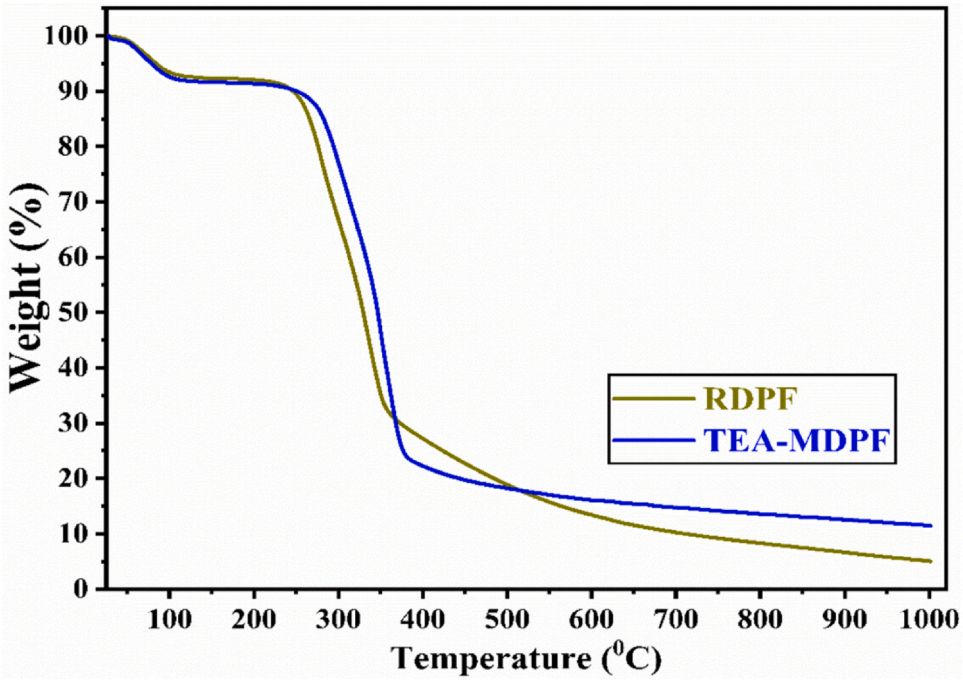

Fig. 4. TGA analysis of date palm biomass (a) RDPF and (b) TEA–MDPF at 10 °C/min.

readily at pH levels lower than pHpzc, as the molecule's anionic surface shows considerable adsorption where the pH was below the pKa of 2,4,6-TCP [45]. When the pH is low, the surface functional groups on the biomass become protonated. This creates a higher electron density on the solute molecules, which increases the adsorption capacity. As the pH increases, the repulsions between negatively charged adsorbent surfaces (RDPF and TEA-MDPF) and the negative charge on the 2,4,6-TCP molecule increase, and their by decreasing the interaction within the solution phase. This results in decreased adsorption capacity at higher pH levels. A similar trend was observed in the adsorption of 2,4,6-TCP onto various adsorbents, including rice husk composite, mango seed shell, organo-montmorillonites, and household waste biomass [46–49]. Both adsorbents showed maximum adsorption capacity at an acidic pH range. Researchers have also reported a high uptake capacity of chlorophenols at low pH [45,50,51]. Therefore, for further adsorption studies, a pH of 2.0 and 6.0 was chosen for the adsorption of 2,4,6-TCP on the RDPF and TEA-MDPF.

3.2.2. *Influence of RDPF and TEA-MDPF dosage*

In this study, the impact of RDPF and TEA-MDPF dose loading on the remediation of 2,4,6-TCP from its solution at 30 °C using various amounts (0.1–1.0 g), an initial concentration of 100 mg/L, an optimum

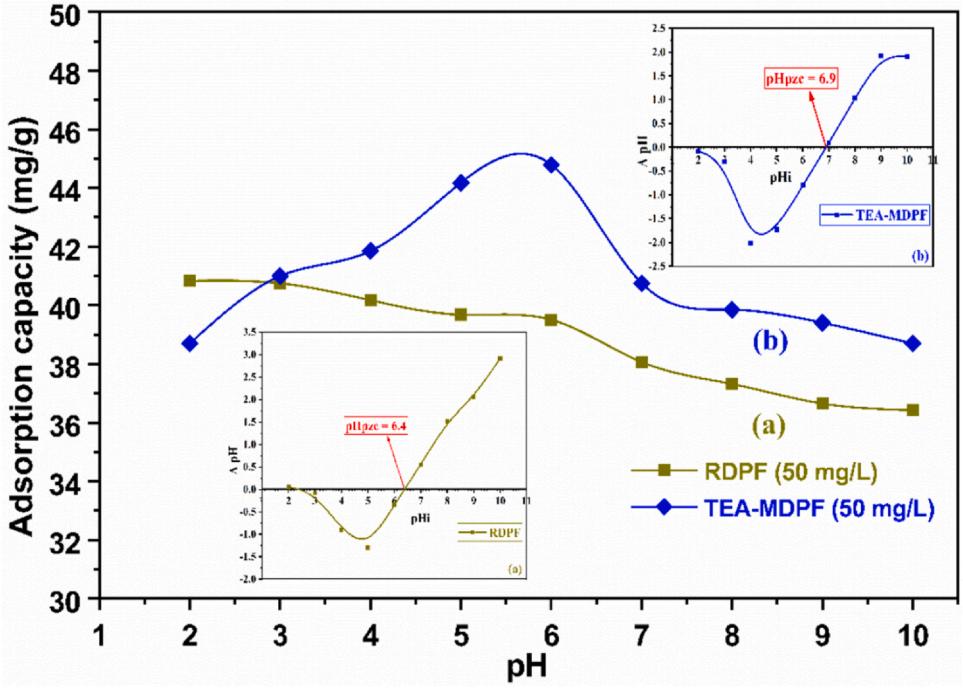

Fig. 5. pH and pHpzc effect on 2,4,6-TCP sorption onto (a) RDPF and (b) TEA–MDPF at 30 ± 1°C (C_0 = 50 mg/L, Agitation rate = 175 rpm, adsorbent dosage = 0.1 g, Contact time = 4 h.

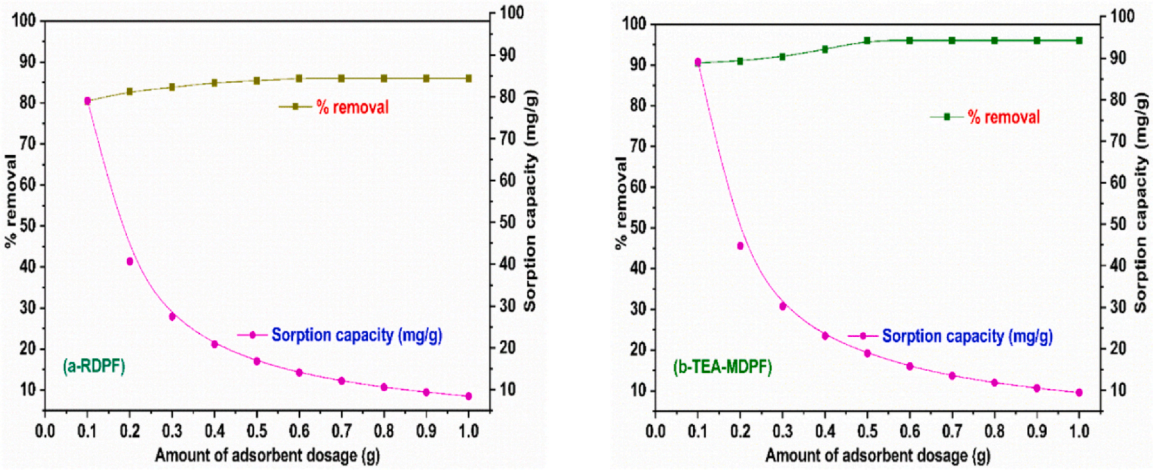

Fig. 6. (a-b). 2,4,6-TCP adsorption onto (a) RDPF and (b) TEA–MDPF biomass dosage at 30 ± 1ºC [Contact time = 4 h, amount of dosage = 0.1 – 0.1 g, C_0 = 100 mg/L, pH = 2.0 and 6.0].

pH 2–6 and a contact time of 4 h. With an increase in the adsorbent mass, both biomass sorption capacities decreased while the removal (%) of 2,4,6-TCP increased, as depicted in Fig. 5(a,b). Fig. 6(a,b) illustrates the percentage removal of 2,4,6-TCP enhanced and the sorption capacity of both biomass decreased with increasing adsorbent mass dose. An adsorbent of 0.5 g, TEA-MDPF, demonstrated the highest removal efficiency of 96 %. Due to excessive active sites associated with the increased biomass dose, the q_e (mg/g) value of 2,4,6-TCP decreases as the RDPF and TEA-MDPF content increases [12,52,53]. As a matter of fact, TEA-MDPF is more effective at eliminating 2,4,6-TCP compared to RDPF biomass. Therefore, 0.6 g and 0.5 g of RDPF and TEA-MDPF were employed as the adsorbent biomass doses in all subsequent experiments to remove 2,4,6-TCP.

3.2.3. *Influence of contact time and initial concentration*

The agitation time significantly affects the 2,4,6-TCP contaminant uptake by RDPF and TEA-MDPF. The impact of the contact time period and the initial 2,4,6-TCP concentration (50–200 mg/L) on the 2,4,6-TCP removal was studied at room temperature (30 °C). Fig. 7(a-b) displays that the increment capacity increases with initial concentration and agitation time. The removal rate of RDPF and TEA-MDPF biomass is initially fast but reaches equilibrium after 120 and 90 min, respectively. The rapid removal rate at the beginning stage of adsorption was due to the superior attraction of the corresponding groups and the accessibility of the exterior surface of the adsorbent. TEA-MDPF exhibits a higher 2,4,6-TCP uptake capacity (q_e) in the range of 50–200 mg/L compared to RDPF [32]. The higher initial concentration results in greater 2,4,6-TCP adsorption due to increased mass transfer driving force. Therefore, we have determined that a contact time of 120 and 90 min is ideal for achieving an equilibrium state during the remediation process of 2,4,6-TCP pollutant from aqueous medium by using RDPF and TEA-MDPF biomass. This timing has proven to be effective for achieving successful results in the remediation process.

3.3. *Adsorption kinetics of 2,4,6-TCP onto RDPF and TEA-MDPF*

In the present study, we conducted a kinetic analysis using two models, namely the PFO (pseudo-first-order) [54] and PSO (pseudo-second-order) models [15,55], to investigate the mechanisms involved in the adsorption of 2,4,6-TCP. Equations 6, 7, 8, and 9 in the supplementary section represent the different kinetic models of PFO, PSO, Intraparticle diffusion [20], and Elovich [56], respectively. In Table 3, you can find the regression correlation coefficients and rate constants for both kinetic models. Based on the low adjusted R^2 values and significant uniformity observed among the experimental (q_e, exp) and computed (q_e, cal) values, it can be concluded that the PFO theory was not suitable for accurately predicting the sorption performance of 2,4,6-TCP on the RDPF and TEA-MDPF adsorbent. However, the PSO kinetic model exhibited better agreement among the experimental and calculated values of (q_e), especially when considering the initial

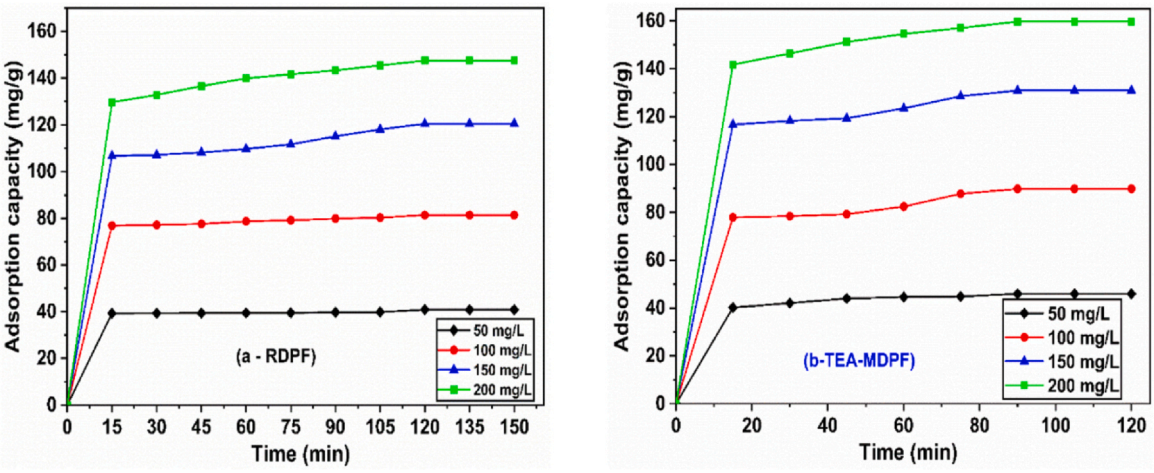

Fig. 7. (a-b). Effect of 2,4,6-TCP sorption onto (a) RDPF and (b) TEA–MDPF shaking time at 30 ± 1ºC [(◆) C_0 = 50 mg/L, (•) C_0 = 100 mg/L, (▲) C_0 = 150 mg/L, (□) C_0 = 200 mg/L; dosage amount = 0.1 g; shaking speed = 175 rpm; Contact time = 3 h, pH = 2.0 & 6.0].

Table 3
PFO and PSO kinetic rate constants of 2,4,6-TCP on RDPF and TEA–MDPF.

2,4,6-TCP - RDPF											
PFO							PSO				
C_0 (mg/L)	$q_{e,\ exp}$ (mg/g)	$q_{e,\ cal}$ (mg/g)	k_1 (min^{-1})	R^2	Δq_t (%)	χ^2	$q_{e,\ cal}$ (mg/g)	k_2 (g/mg/min)	R^2	Δq_t (%)	χ^2
50	40.88	1.77	0.004	0.903	106.87	35,389.96	39.93	0.052	1.000	0.63	0.011
100	81.43	6.79	0.018	0.958	87.93	12,024.81	81.11	0.008	0.999	1.55	0.14
150	120.52	17.17	0.008	0.940	94.19	15,169.44	119.80	0.002	0.997	4.26	1.50
200	147.55	28.68	0.022	0.967	86.11	5884.39	148.81	0.002	0.999	2.42	0.57
2,4,6-TCP - TEA Modified Date Palm Fiber (TEA-MDPF)											
50	45.93	8.34	0.028	0.959	87.23	1405.80	46.37	0.008	0.999	0.97	0.19
100	89.87	23.90	0.026	0.714	81.46	1645.18	89.84	0.002	0.993	4.68	0.92
150	130.89	28.22	0.027	0.783	84.88	3236.76	131.34	0.002	0.997	3.35	0.69
200	159.66	32.33	0.031	0.981	85.06	3960.02	161.81	0.002	0.999	1.67	0.21

Table 4
Kinetic (IDM and EKM) rate constants of 2,4,6-TCP on RDPF and TEA–MDPF.

2,4,6-TCP – Raw Date Palm Fiber (RDPF)													
IDM								EKM					
Conc (mg/L)	$q_{e,\ exp}$ (mg/g)	$q_{e,\ cal}$ (mg/g)	k_{id}	C	R^2	Δq_t (%)	χ^2	q $_{(e,\ cal)}$ (mg/g)	(1/b)ln (ab) (mg/g)	1/b (mg/g)	R^2	Δq_t (%)	χ^2
50	40.88	39.76	0.08	38.90	0.854	0.18	0.01	39.72	38.51	0.25	0.752	0.23	0.01
100	81.43	80.20	0.58	74.23	0.956	0.33	0.01	79.93	71.28	1.85	0.890	0.53	0.02
150	120.52	115.81	1.78	97.99	0.847	1.38	0.15	114.86	89.89	5.36	0.737	1.81	0.26
200	147.55	145.57	2.52	119.73	0.994	0.28	0.01	144.54	106.13	8.25	0.974	0.63	0.04
2,4,6-TCP – TEA Modified Date Palm Fiber (TEA–MDPF)													
50	45.93	35.56	1.01	36.56	0.946	0.92	0.01	45.12	31.97	3.04	0.974	0.63	0.01
100	89.87	85.25	1.87	69.01	0.751	2.21	0.20	84.56	62.19	5.18	0.652	2.60	0.28
150	130.89	126.31	2.33	106.05	0.845	1.38	0.12	125.53	97.15	6.57	0.758	1.72	0.18
200	159.66	157.26	3.26	128.94	0.997	0.19	0.01	156.45	114.88	9.62	0.983	0.48	0.02

concentration of 2,4,6-TCP (C_0 = 50–200 mg/L) in the current study. This is also reflected in the improved regression coefficients (R^2), thus confirming the preeminence of the PSO kinetics over the PFO kinetics for estimating the adsorption of 2,4,6-TCP using the RDPF and TEA-MDPF biomass.

The intra-particle diffusion (ID) model assesses how significant the mass transport of the solute. Table 4 shows the calculated k_{id}, intercept, and R^2 values. If Eq. 9 results in a linear profile via the origin, then ID is the main rate-controlling limiting step. However, in RDPF and TEA-MDPF biomass, the intercept ranges are not valid. An effective intercept suggests that the sorption mainly takes place on the surface of the sorbent. During the migration of the solute from the liquid phase to the external surface of the sorbent, the mass transport is regulated by external mass transport resistance. To determine the contaminant uptake rate, the Elovich model is also utilized. Although it doesn't suggest any definite mechanism that regulates the sorbent and sorbent contact, the model assumes that the surface of the adsorbent is actively heterogeneous. However, as shown in Table 4, the computed q_e values of the Elovich model do not fit with the equilibrium data.

In the present study, the PFO, PSO, Elovich, and intraparticle diffusion kinetic equations were compared to determine which model delivers the best description of the sorption of 2,4,6-TCP onto RDPF and TEA-MDPF. The model and experimental results for concentrations ranging from 50–200 mg/L of 2,4,6-TCP were depicted in the supplementary Figs. S7(a–d) and S8(e–h). The experimental data matched the PSO kinetic model, whereas the PFO kinetics failed to give a sufficient explanation of the sorption of 2,4,6-TCP onto RDPF and TEA-MDPF. Different models data fitted with 2,4,6-TCP adsorption on RDPF and TEA-MDPF are inserted in Tables 3 and 4, along with their corresponding Chi-square (χ^2), Δq_t (%), and regression (R^2) values. The PSO model had a greater R^2 value, which was higher than 0.993 and near unity than those of the Elovich, PFO, and intraparticle diffusion. In the employment of PSO, the computed (q_e, cal) values displayed a good fit with the experimental values (q_t, exp). Therefore, the examined data reveals the PSO kinetic model agrees well with 2,4,6-TCP adsorption on RDPF and TEA-MDPF. This is consistent with the new findings that have revealed the kinetics of 2,4,6-TCP sorption onto different adsorbents and also suggested PSO kinetic models [13,50,56].

3.4. Adsorption isotherm models

Understanding the diffusion of sorbate molecules between solid and liquid phases during the equilibrium conditions of the sorption is essential. Adsorption isotherm plays a crucial role in explaining this process. In this course, Langmuir (Eq.10), Freundlich (Eq.11), and Dubinin–Radushkevich (Eq.13) models [12,21,57] were used to analyze the equilibrium adsorption isotherm, which is shown in the supplementary section 3.5. Equibrilium Langmuir isotherm model was used to identify the adsorption process for monolayer through physical forces. The RDPF and TEA-MDPF monolayers displayed the highest adsorption capacity (q_m) of 115.50 and 191.75 mg/g, respectively. Alternatively, the isotherm Freundlich model was employed to evaluate the multilayer sorption process by chemical mode on heterogeneous surfaces. Dubinin-Radushkevich (D-R) isotherm model was tested to find out if the sorption process was chemisorption or physical adsorption. The parameter E was used to characterize the type of the sorption method used in this study. Typically, for the physical adsorption, the E value exhibits less than 8 kJ/mol, whereas for the adsorption of ion exchange, the E values ranges between 8–16 kJ/mol. Table 5 presents the RDPF and TEA-MDPF parameter values of correlation coefficients (R^2), Chi-square (χ^2), and standard deviation (Δq_e (%)) for all three isotherms, i.e., Langmuir, Freundlich, and D-R. The RDPF and TEA-MDPF

Table 5
Isotherm Parameters of 2,4,6-TCP on RDPF and TEA–MDPF.

Adsorbate	Langmuir					Freundlich					D-R (Dubinin- Radushkevich)				
	RDPF														
	q_m (mg/g)	b (L/mg)	R^2	Δq_e (%)	χ^2	K_F ((mg/g) $(L/mg)^{1/n}$)	n	R^2	Δq_e (%)	χ^2	q_s (mmol/g)	E (kJ/mol)	R^2	Δq_e (%)	χ^2
2,4,6-TCP	115.50	0.026	0.994	11.23	7.10	3.335	1.189	0.991	6.66	1.67	4.89	8.53	0.986	8.32	2.65
	TEA–MDPF														
2,4,6-TCP	191.75	0.027	0.997	6.99	3.19	5.405	1.134	0.997	3.35	0.50	4.31	8.51	0.995	4.96	1.11

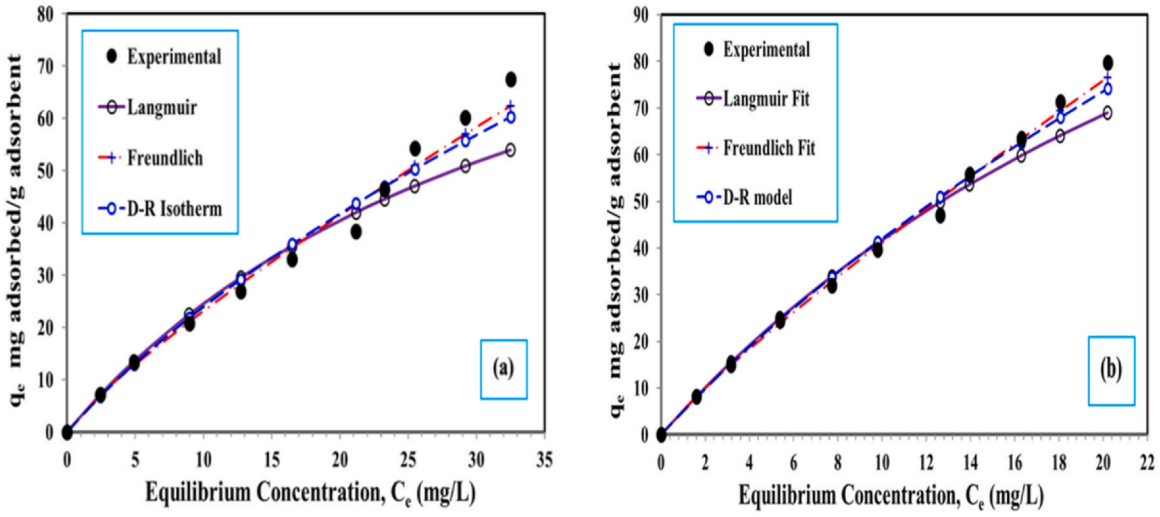

Fig. 8. Experimental and theoretical parameter values of (a) RDPF and (b) TEA–MDPF adsorbents from the Freundlich, Langmuir, and D-R isotherm models.

determinations of all three isotherm models are in agreement with the experimental data, as represented in Fig. 8(a-b). Based on the results, the Freundlich isotherm model demonstrated a better fit with the experimental sorption data than the D-R and Langmuir isotherm models. In specific, the TEA-MDPF Freundlich isotherm model showed the highest R^2 (0.997), lowest Δq_e (%) (3.35), and lowest Chi-square (χ^2) value (0.50) among the three isotherm models analyzed.

3.5. Comparison with other literature

Table 6 provides a summary of data from various 2,4,6-TCP adsorption systems that use different types of adsorbents. Comparing the findings of this study to those of previous similar studies, it is evident that TEA-MDPF has the highest potential as an effective adsorbent for 2,4,6-TCP removal. In fact, TEA-MDPF has a higher removal capacity than most of the biomasses listed in Table 6 and even exceeds that of activated biomasses. Additionally, RDPF could be a promising adsorbent compared to many other adsorbents.

3.6. Cost-effective Comparison Analysis

To use adsorption techniques on a large scale, it is important to analyze the cost implications of preparing the adsorbent. The cost of the activated carbon can be obtained via several factors, such as the price of the precursor, the cost of activating the agent, and the cost of using essential equipment. Date palm biomass (Date palm fiber (DPF)), which is prepared

Table 6
Comparison of different adsorbents used for the remediation process of 2,4,6-TCP onto RDPF and TEA–MDPF.

Adsorbent	Q^0 (mg/g)	pH	Time (hr)	Ref
Zn^{2+}- Al^{3+} -$C_4H_4O_6^{2-}$-LDHs	599.6	3	2.5	[1]
Pine Bark Powder	289.09	6	2	[2]
p-DMAC4/GO	38.4	6	1	[13]
Acacia leucocephala bark	256.4	5	3	[15]
FAC & ATFAC	49.80 &101	2	24	[50]
Cannaindica	52.08	4	20 days	[51]
GO – PVPP	466.77	4	-	[52]
Hal nanocomposites	196.08	3	10	[53]
Bentonite modified with benzyl dimethyl tetra decyl ammonium chloride	35	4	1	[58]
Azollafiliculoides biomass	6.2	5	2	[59]
Surfactant modified Bentonite	13.9	3	6	[60]
Chemically modified chitosan CS-SA-CD	375.94	5	1.5	[61]
Sargassum Boveanum Macroalgae (MA & BCM)	10 & 175	5	6	[62]
RDPF	115.50	2	2	This study
TEA-MDPF	191.75	6	1.5	This study

Table 7
Approximate cost-effective production of date palm biomass.

Date Palm biomass – 1 Kg	
Material input (Biomass production)	Amount /Cost ($/kg)
Precursor material	0.02*
Transportation	0.10
Processing #	0.70
Material output final cost (Kg)	0.82

Processing includes Collection of raw materials, Transportation, Shredding, Washing and Drying, Crushing and Sieving, Ball milling, and various Chemical treatments and manpower.

* Based on the reported cost in reference [66–68], the cost may vary slightly if inflation over the years is taken into consideration.

from readily existing agricultural waste, is a cost-effective option. Table 7 provides a detailed cost incurred in preparing 1 kg of date palm biomass compared to date palm biochar (DBC), wood-based activated carbon (AC), and presented commercially activated carbon (CAC). From the cost assessment, it has been established that date palm biomass is less expensive compared to other adsorbents like DBC, AC, and CAC. Based on these cost assumptions, we are optimistic that date palm biomass adsorbent is a more cost-effective alternative to date palm biochar (DBC), activated carbon derived from wood (AC), and CAC [63–65].

4. Conclusions

In this study, researchers prepared two types of adsorbents from date palm agro-waste: RDPF and TEA-MDPF. The sorption isotherms and kinetics for the remediation of 2,4,6-TCP from an aqueous media. The researchers found that solution pH affected the sorption capacity. RDPF exhibited a better sorption capacity at pH 2.0, while TEA-MDPF showed higher adsorption capacity at pH 6.0, with no increase in capacity beyond that pH. The chemical modification improved the removal capability of TEA-MDPF for 2,4,6-TCP with an efficiency removal of up to 95 %. The kinetic adsorption results for both RDPF and TEA-MDPF followed PSO kinetics. The researchers found that the Freundlich equilibrium isotherm model was better at describing the heterolayer sorption of 2,4,6-TCP onto the RDPF and TEA-MDPF. The Langmuir model described the monolayer maximum sorption capacities (q_{max}) of 115.50 and 191.75 mg/g, respectively. Researchers should explore cost-effective processing methods to extract specific properties from readily available agricultural waste, thereby supporting the economic growth of countries. Overall, the study showed that RDPF and TEA-MDPF can be utilized as stable, inexpensive, and practical adsorbents for the remediation of 2,4,6-TCP in wastewater. Researchers are planning to conduct further studies on the employment of date palm fiber in wastewater treatment.

CRediT authorship contribution statement

Nadavala Siva Kumar: Conceptualization, Methodology, Investigation, Supervision, Formal analysis, Writing – original draft, Funding acquisition, Writing – review & editing. **Mohammad Asif:** Supervision, Validation, Writing – review & editing. **Anesh Manjaly Poulose:** Visualization, Formal analysis. **Ebrahim H. Al-Ghurabi:** Software, Formal analysis. **Shaddad S. Alhamedi:** Data curation, Software, Formal analysis. **Janardhan Reddy Koduru:** Validation, Writing – review & editing.

Data Availability

Data will be made available on request.

Declaration of Competing Interest

The authors declare that they have no known competing financial interests or personal relationships that could have appeared to influence the work reported in this paper.

Acknowledgments

This Project was funded by the National Plan for Science, Technology, and Innovation (MAARIFAH), King Abdulaziz City for Science and Technology, Kingdom of Saudi Arabia, Award Number (2-17-01-001-0064).

Appendix A. Supporting information

Supplementary data associated with this article can be found in the online version at doi:10.1016/j.dwt.2024.100405.

References

[1] Su T, Gao W, Gao Y, Ma X, Gao L, Song Y. The application of response surface methodology for 2,4,6-trichlorophenol removal from aqueous solution using synthesized zn2+-al3+-tartrate layered double hydroxides. Processes 2022;10:282. https://doi.org/10.3390/pr10020282.
[2] Kumar NS, Asif M, Al-Hazzaa MI, Ibrahim AA. Biosorption of 2,4,6-trichlorophenol from aqueous medium using agro-waste: Pine (Pinus densiflora Sieb) bark powder. Acta Chim Slov 2018;65:221–30. https://doi.org/10.17344/acsi.2017.3886.
[3] Ghanbari F, Moradi M, Gohari F. Degradation of 2,4,6-trichlorophenol in aqueous solutions using peroxymonosulfate/activated carbon/UV process via sulfate and hydroxyl radicals. J Water Process Eng 2016;9:22–8. https://doi.org/10.1016/j.jwpe.2015.11.011.
[4] Kwon G, Bhatnagar A, Wang H, Kwon EE, Song H. A review of recent advancements in utilization of biomass and industrial wastes into engineered biochar. J Hazard Mater 2020;400:123242. https://doi.org/10.1016/j.jhazmat.2020.123242.
[5] Radhika M, Palanivelu K. Adsorptive removal of chlorophenols from aqueous solution by low cost adsorbent-Kinetics and isotherm analysis. J Hazard Mater 2006;138:116–24. https://doi.org/10.1016/j.jhazmat.2006.05.045.
[6] Demissie H, An G, Jiao R, Ma G, Liu L, Sun H, Wang D. Removal of phenolic contaminants from water by in situ coated surfactant on Keggin-aluminum nanocluster and biodegradation. Chemosphere 2021;269:128692. https://doi.org/10.1016/j.chemosphere.2020.128692.
[7] Kruanak K, Jarusutthirak C. Degradation of 2,4,6-trichlorophenol in synthetic wastewater by catalytic ozonation using alumina supported nickel oxides. J Environ Chem Eng 2019;7:102825. https://doi.org/10.1016/j.jece.2018.102825.
[8] Caetano M, Valderrama C, Farran A, Cortina JL. Phenol removal from aqueous solution by adsorption and ion exchange mechanisms onto polymeric resins. J Colloid Interface Sci 2009;338:402–9. https://doi.org/10.1016/j.jcis.2009.06.062.
[9] Liu L, Wang J, Yang H, Gao D, Cui Y, Chen H, Qin Y, Ye R, Ding X. The critical impacts of pyrochar during 2,4,6-trichlorophenol photochemical remediation process: Cooperation between persistent free radicals and oxygenated functional groups. Environ Pollut 2023;330:121813. https://doi.org/10.1016/j.envpol.2023.121813.
[10] Hernández-Del Castillo PC, Oliva J, Núñez-Luna BP, Rodríguez-González V. Novel polypropylene-TiO2:Bi spherical floater for the efficient photocatalytic degradation of the recalcitrant 2,4,6-TCP herbicide. J Environ Manag 2023;329. https://doi.org/10.1016/j.jenvman.2022.117057.
[11] Zada A, Khan M, Khan MA, Khan Q, Habibi-Yangjeh A, Dang A, Maqbool M. Review on the hazardous applications and photodegradation mechanisms of chlorophenols over different photocatalysts. Environ Res 2021;195:110742. https://doi.org/10.1016/j.envres.2021.110742.
[12] Kumar NS, Asif M, Poulose AM, Suguna M, Al-Hazza MI. Equilibrium and kinetic studies of biosorptive removal of 2,4,6-trichlorophenol from aqueous solutions using untreated agro-waste pine cone biomass. Processes 2019;7. https://doi.org/10.3390/pr7100757.
[13] Hyder A, Thebo M, Janwery D, Buledi JA, Chandio I, Khalid A, Al-Anzi BS, Almukhlifi HA, Thebo KH, Memon FN, Memon AA, Solangi AR, Memon S. Fabrication of para-dimethylamine calix[4]arene functionalized self-assembled graphene oxide composite material for effective removal of 2, 4, 6-tri-Cholorphenol from aqueous environment. Heliyon 2023;9:e19622. https://doi.org/10.1016/j.heliyon.2023.e19622.
[14] Kuśmierek K, Świątkowski A, Dąbek L. Removal of 2, 4, 6-trichlorophenol from aqueous solutions using agricultural waste as low-cost adsorbents. Environ Prot Eng 2017;43:149–63. https://doi.org/10.5277/epel70412.
[15] Siva Kumar N, Woo HS, Min K. Equilibrium and kinetic studies on biosorption of 2,4,6-trichlorophenol from aqueous solutions by Acacia leucocephala bark. Colloids Surf B Biointerfaces 2012;94:125–32. https://doi.org/10.1016/j.colsurfb.2012.01.048.
[16] Kumar NS, Min K. Phenolic compounds biosorption onto Schizophyllum commune fungus: FTIR analysis, kinetics and adsorption isotherms modeling. Chem Eng J 2011;168:562–71. https://doi.org/10.1016/j.cej.2011.01.023.

[17] Jabeen A, Kamran U, Noreen S, Park SJ, Bhatti HN. Mango seed-derived hybrid composites and sodium alginate beads for the efficient uptake of 2,4,6-trichlorophenol from simulated wastewater. Catalysts 2022;12. https://doi.org/10.3390/catal12090972.

[18] Ouafi R, Omor A, Gaga Y, Akhazzane M, Taleb M, Rais Z. Pine cone powder for the adsorptive removal of copper ions from water. Chem Ind Chem Eng Q 2021;27:341–54. https://doi.org/10.2298/CICEQ200101001O.

[19] Lee BG, Rowell RM. Removal of heavy metal ions from aqueous solutions using lignocellulosic fibers. J Nat Fibers 2004;1:97–108. https://doi.org/10.1300/J395v01n01_07.

[20] Nadavala SK, Che Man H, Woo H-S. Biosorption of phenolic compounds from aqueous solutions using pine (pinus densiflora sieb) bark powder. BioResources 2014;9:5155–74. https://doi.org/10.15376/biores.9.3.5155-5174.

[21] Siva Kumar N, Asif M, Poulose AM, Al-Ghurabi EH, Alhamedi SS, Koduru JR. Preparation, characterization, and chemically modified date palm fiber waste biomass for enhanced phenol removal from an aqueous environment. Mater (Basel) 2023;16. https://doi.org/10.3390/ma16114057.

[22] El-Bery HM, Saleh M, El-Gendy RA, Saleh MR, Thabet SM. High adsorption capacity of phenol and methylene blue using activated carbon derived from lignocellulosic agriculture wastes. Sci Rep 2022;12:1–17. https://doi.org/10.1038/s41598-022-09475-4.

[23] Al Arni S, Elwaheidi M, Converti A, Benaissa M, Salih AAM, Ghareba S, Abbas N. Application of date palm surface fiber as an efficient biosorbent for wastewater treatment. ChemBioEng Rev 2023;10:55–64. https://doi.org/10.1002/cben.202200008.

[24] Shafiq M, Alazba AA, Amin MT. Removal of heavy metals from wastewater using date palm as a biosorbent: a comparative review. Sains Malays 2018;47:35–49. https://doi.org/10.17576/jsm-2018-4701-05.

[25] Al-Haidary AMA, Zanganah FHH, Al-Azawi SRF, Khalili FI, Al-Dujaili AH. A study on using date palm fibers and leaf base of palm as adsorbents for Pb(II) ions from its aqueous solution. Water Air Soil Pollut 2011;214:73–82. https://doi.org/10.1007/s11270-010-0405-1.

[26] Amin MT, Alazba AA, Amin MN. Absorption behaviours of copper, lead, and arsenic in aqueous solution using date palm fibres and orange peel: Kinetics and thermodynamics. Pol J Environ Stud 2017;26:543–57. https://doi.org/10.15244/pjoes/66963.

[27] Alghamdi AA. An investigation on the use of date palm fibers and coir pith as adsorbents for Pb(II) ions from its aqueous solution. Desalin Water Treat 2016;57:12216–26. https://doi.org/10.1080/19443994.2015.1048743.

[28] Melliti A, Yılmaz M, Sillanpää M, Hamrouni B, Vurm R. Low-cost date palm fiber activated carbon for effective and fast heavy metal adsorption from water: Characterization, equilibrium, and kinetics studies. Colloids Surf A Physicochem Eng Asp 2023;672. https://doi.org/10.1016/j.colsurfa.2023.131775.

[29] Alshabanat M, Al-Mufarij RS, Al-Senani GM. Study on adsorption of malachite green by date palm fiber. Orient J Chem 2016;32:3139–44. https://doi.org/10.13005/ojc/320636.

[30] Alshabanat M, Alsenani G, Almufarij R. Removal of crystal violet dye from aqueous solutions onto date palm fiber by adsorption technique. J Chem 2013;2013. https://doi.org/10.1155/2013/210239.

[31] Ali QA, Shaban MAA, Mohammed SJ, M-Ridha MJ, Abd-Almohi HH, M. Abed K, Salleh MZM, Hasan HA. Date Palm Fibre Waste Exploitation for the Adsorption of Congo Red Dye via Batch and Continuous Modes. J Ecol Eng 2023;24:259–76. https://doi.org/10.12911/22998993/169176.

[32] Alminderej FM, Younis AM, Albadri AEAE, El-Sayed WA, El-Ghoul Y, Ali R, Mohamed AMA, Saleh SM. The superior adsorption capacity of phenol from aqueous solution using Modified Date Palm Nanomaterials: A performance and kinetic study. Arab J Chem 2022;15:104120. https://doi.org/10.1016/j.arabjc.2022.104120.

[33] Bentarfa D, Sekirifa ML, Hadj-Mahammed M, Richard D, Pallier S, Khaldoun B, Belkhalfa H, Al-Dujaili AH. Characterization of activated carbon prepared from date palm fibers by physical activation for the removal of phenol from aqueous solutions. Desalin Water Treat 2021;236:190–202. https://doi.org/10.5004/dwt.2021.27711.

[34] Habchi A, Dahou ME, Slimani S, Kalloum S. Removal of Nitrate from Wastewater by Adsorption on Date Palm Waste (DPW). J Environ Treat Tech 2023;11:75–81.

[35] Song Y, Ding S, Chen S, Xu H, Mei Y, Ren J. Removal of malachite green in aqueous solution by adsorption on sawdust. Korean J Chem Eng 2015;32:2443–8. https://doi.org/10.1007/s11814-015-0103-1.

[36] Daffalla SB, Mukhtar H, Shaharun MS. Preparation and characterization of rice husk adsorbents for phenol removal from aqueous systems. PLoS One 2020;15. https://doi.org/10.1371/journal.pone.0243540.

[37] Wang Y, Jiang W, Tang Y, Liu Z, Qin Q, Xu Y. Biochar–supported sulfurized nanoscale zero–valent iron facilitates extensive dechlorination and rapid removal of 2,4,6–trichlorophenol in aqueous solution. Chemosphere 2023;332:138835. https://doi.org/10.1016/j.chemosphere.2023.138835.

[38] Stjepanović M, Velić N, Lončarić A, Gašo-Sokač D, Bušić V, Habuda-Stanić M. Adsorptive removal of nitrate from wastewater using modified lignocellulosic waste material. J Mol Liq 2019;285:535–44. https://doi.org/10.1016/j.molliq.2019.04.105.

[39] Bai RS, Abraham TE. Studies on enhancement of Cr(VI) biosorption by chemically modified biomass of Rhizopus nigricans. Water Res 2002;36:1224–36. https://doi.org/10.1016/S0043-1354(01)00330-X.

[40] Thamilarasi MJV, Anilkumar P, Theivarasu C, Sureshkumar MV. Removal of vanadium from wastewater using surface-modified lignocellulosic material. Environ Sci Pollut Res 2018;25:26182–91. https://doi.org/10.1007/s11356-018-2675-x.

[41] Inayat A, Jamil F, Ahmed SF, Ayoub M, Abdul PM, Aslam M, Mofijur M, Khan Z, Mustafa A. Thermal degradation characteristics, kinetic and thermodynamic analyses of date palm surface fibers at different heating rates. Fuel 2023;335:127076. https://doi.org/10.1016/j.fuel.2022.127076.

[42] Raza M, Abu-Jdayil B, Al-Marzouqi AH, Inayat A. Kinetic and thermodynamic analyses of date palm surface fibers pyrolysis using Coats-Redfern method. Renew Energy 2022;183:67–77. https://doi.org/10.1016/j.renene.2021.10.065.

[43] Saba N. Date Palm Fiber Composites. Singapore: Springer Singapore,; 2020. https://doi.org/10.1007/978-981-15-9339-0.

[44] Kumar NS, Asif M, Poulose AM, Al-Ghurabi EH, Alhamedi SS, Koduru JR. Remediation of 2,4,6-trichlorophenol from aqueous solution by raw and chemical modified date palm stone biomass: Kinetics and isotherms studies. BioResources 2024;19:3543–70. https://doi.org/10.15376/biores.19.2.3543-3570.

[45] Sahnoun S, Boutahala M, Zaghouane-Boudiaf H, Zerroual L. Trichlorophenol removal from aqueous solutions by modified halloysite: kinetic and equilibrium studies. Desalin Water Treat 2016;57:15941–51. https://doi.org/10.1080/19443994.2015.1075159.

[46] Noor A, Khan A, Bhatti HN, Zahid M, Aslam F, Naouar A, Al-Fawzan FF, Alissa SA, Iqbal M. Polypyrrole and rice husk composite potential for the adsorptive removal of 2,4,6-trichloro phenol from aqueous medium. Arab J Chem 2022;15:104352. https://doi.org/10.1016/j.arabjc.2022.104352.

[47] Jabeen A, Bhatti HN, Noreen S, Gaffar A. Adsorptive removal of 2, 4, 6-trichlorophenol from wastewater by mango seed shell and its magnetic composites: batch and column study. Int J Environ Anal Chem 2023;103:5639–59. https://doi.org/10.1080/03067319.2021.1941916.

[48] Yang Q, Gao M, Zang W. Comparative study of 2,4,6-trichlorophenol adsorption by montmorillonites functionalized with surfactants differing in the number of head group and alkyl chain. Colloids Surf A Physicochem Eng Asp 2017;520:805–16. https://doi.org/10.1016/j.colsurfa.2017.02.057.

[49] Ouadjenia F, Marouf R, Berrazoum A. Valorisation of household waste biomass as a bio-adsorbent of 2,4,6-trichlorophenol from aqueous medium. Int J Environ Stud 2019;76:471–90. https://doi.org/10.1080/00207233.2019.1585155.

[50] Priyanka O, Sudesh R, Kunwar S. Modified coconut fiber used as adsorbent for the removal of 2-chlorophenol and 2,4,6-trichlorophenol from aqueous solution. South Afr J Chem Eng 2014;19:1–21.

[51] Enyoh CE, Isiuku BO. 2,4,6-Trichlorophenol (TCP) removal from aqueous solution using Canna indica L.: kinetic, isotherm and Thermodynamic studies. Chem Ecol 2021;37:64–82. https://doi.org/10.1080/02757540.2020.1821673.

[52] Lv X, Li S. Graphene Oxide-Crospolyvinylpyrrolidone Hybrid Microspheres for the Efficient Adsorption of 2,4,6-Trichlorophenol. ACS Omega 2020;5:18862–71. https://doi.org/10.1021/acsomega.0c02028.

[53] Zango ZU, Garba ZN, Abu Bakar NHH, Tan WL, Abu Bakar M. Adsorption studies of Cu2 +–Hal nanocomposites for the removal of 2,4,6-trichlorophenol. Appl Clay Sci 2016;132–133:68–78. https://doi.org/10.1016/j.clay.2016.05.016.

[54] Ilyas M, Liao Y, Xu J, Wu S, Liao W, Zhao X. Removal of anthracene from vehicle-wash wastewater through adsorption using eucalyptus wood waste-derived biochar. Desalin Water Treat 2024;317:100115. https://doi.org/10.1016/j.dwt.2024.100115.

[55] Sharain-Liew YL, Joseph CG, How SE. Biosorption of lead contaminated wastewater using cattails (Typha angustifolia) leaves: Kinetic studies. J Serb Chem Soc 2011;76:1037–47. https://doi.org/10.2298/JSC100628084L.

[56] Kumar NS, Shaikh HM, Asif M, Al-Ghurabi EH. Engineered biochar from wood apple shell waste for high-efficient removal of toxic phenolic compounds in wastewater. Sci Rep 2021;11. https://doi.org/10.1038/s41598-021-82277-2.

[57] Liu L, Luo XB, Ding L, Luo SL. Application of Nanotechnology in the Removal of Heavy Metal From Water. Elsevier Inc.,; 2018. https://doi.org/10.1016/B978-0-12-814837-2.00004-4.

[58] Ghezali S, Mahdad-Benzerdjeb A, Ameri M, Bouyakoub AZ. Adsorption of 2,4,6-trichlorophenol on bentonite modified with benzyldimethyltetradecylammonium chloride. Chem Int 2019;4:24–32.

[59] Zazouli MA. Application of Azolla for 2, 4, 6-Trichlorophenol (TCP) Removal from Aqueous Solutions. Arch Hyg Sci 2013;2:143–9.

[60] Anirudhan TS, Ramachandran M. Removal of 2,4,6-trichlorophenol from water and petroleum refinery industry effluents by surfactant-modified bentonite. J Water Process Eng 2014;1:46–53. https://doi.org/10.1016/j.jwpe.2014.03.003.

[61] Zhou LC, Meng XG, Fu JW, Yang YC, Yang P, Mi C. Highly efficient adsorption of chlorophenols onto chemically modified chitosan. Appl Surf Sci 2014;292:735–41. https://doi.org/10.1016/j.apsusc.2013.12.041.

[62] Nazal MK, Gijjapu D, Abuzaid N. Study on adsorption performance of 2,4,6-trichlorophenol from aqueous solution onto biochar derived from macroalgae as an efficient adsorbent. Sep Sci Technol 2021;56:2183–93. https://doi.org/10.1080/01496395.2020.1815778.

[63] Shaheen J, Fseha YH, Sizirici B. Performance, life cycle assessment, and economic comparison between date palm waste biochar and activated carbon derived from woody biomass. Heliyon 2022;8:e12388. https://doi.org/10.1016/j.heliyon.2022.e12388.

[64] Yahya SAl, Iqbal T, Omar MM, Ahmad M. Techno-economic analysis of fast pyrolysis of date palm waste for adoption in Saudi Arabia. Energies 2021;14. https://doi.org/10.3390/en14196048.

[65] Bello OS, Alao OC, Alagbada TC, Agboola OS, Omotoba OT, Abikoye OR. A renewable, sustainable and low-cost adsorbent for ibuprofen removal. Water Sci Technol 2021;83:111–22. https://doi.org/10.2166/wst.2020.551.

[66] Faiad A, Alsmari M, Ahmed MMZ, Bouazizi ML, Alzahrani B, Alrobei H. Date palm tree waste recycling: treatment and processing for potential engineering applications. Sustain 2022;14. https://doi.org/10.3390/su14031134.

[67] Al-Oqla FM, Sapuan SM. Natural fiber reinforced polymer composites in industrial applications: Feasibility of date palm fibers for sustainable automotive industry. J Clean Prod 2014;66:347–54. https://doi.org/10.1016/j.jclepro.2013.10.050.

[68] Mallaki M, Fatehi R. Design of a biomass power plant for burning date palm waste to cogenerate electricity and distilled water. Renew Energy 2014;63:286–91. https://doi.org/10.1016/j.renene.2013.09.036.